Direct Arylation Polycondensation for Synthesis of Bithiazole-based Conjugated Polymers and Their Physical Properties

Junpei Kuwabara,[1] Masahiro Kuramochi,[1] Songlin Liu,[1] Takeshi Yasuda,[2] Takaki Kanbara[1]

1 Tsukuba Research Center for Interdisciplinary Materials Science (TIMS), Graduate School of Pure and Applied Sciences, University of Tsukuba, 1-1-1 Tennodai, Tsukuba, Ibaraki, 305-8573, Japan.
2 Research Center for Functional Materials, National Institute for Materials Science (NIMS), 1-2-1 Sengen, Tsukuba, Ibaraki 305-0047, Japan

Email: kuwabara@ims.tsukuba.ac.jp, kanbara@ims.tsukuba.ac.jp

ABSTRACT

Reaction conditions of direct arylation polycondensation were investigated for the synthesis of bithiazole-based conjugated polymers, which were difficult to synthesize under previous conditions due to low solubility of the product in the reaction solvent. The investigation revealed that the reaction with Pd(PCy$_3$)$_2$ as a precatalyst and N,N-diethylpropanamide as the reaction solvent afforded three kinds of the bithiazole-based conjugated polymers with high molecular weights. These conditions also effectively suppressed the formation of structural defects, such as a non-alternating structure caused by homo-coupling. The structure–property relations of the obtained polymers were evaluated in terms of absorption properties, energy levels, crystallinity, and semiconducting properties. HOMO/LUMO levels reasonably reflect their chemical structure. High crystallinity of the polymers was confirmed by X-ray diffraction analysis. These polymers tend to aggregate even in the solution state. The control of aggregation characteristics was a key factor for increasing the power conversion efficiency of the organic photovoltaic devices fabricated from the polymers. This study expanded the application range of direct arylation polycondensation for preparation of crystalline polymer materials.

Keywords
Conjugated polymer/ polycondensation/ direct arylation/ bithiazole/ crystallinity/ organic photovoltaics

Running Head
Direct arylation polycondensation

INTRODUCTION

Bithiazole derivatives are attractive aromatic units for optoelectronic materials owing to their planar structure, electron acceptor properties, and strong intermolecular interactions.[1] Bithiazole-based small molecules serve as high-performance n-type semiconducting materials for organic field-effect transistors (OFETs).[2] π-Conjugated polymers bearing bithiazole units have also been reported as n-type semiconducting materials[3] as well as p-type semiconducting materials for OFETs[4,5] and organic photovoltaics (OPVs).[1,6–8] Owing to the weak acceptor property of bithiazole units, bithiazole-based polymers have lower highest occupied molecular orbital (HOMO) levels than corresponding thiophene-based polymers. The low HOMO level of the bithiazole-based polymer provides several advantages in terms of air-stability and electron transporting properties.[1,3–5] In addition, intermolecular interactions between S and N atoms imply that bithiazole-based polymers tend to have strong interchain interactions providing aggregation properties and high crystallinity.

These bithiazole-based polymers have been mainly synthesized by polycondensation using cross-coupling reactions such as the Migita-Kosugi-Stille and Suzuki-Miyaura coupling reactions.[1,9,10] However, instability of the stannylated bithiazole monomer lead to the formation of a low-molecular-weight polymer.[3,11] In recent years, polycondensation using a direct C–H arylation reaction was developed as an alternative method for the synthesis of conjugated polymers.[12–18] Since direct arylation polycondensation does not require organometallic monomers, this new method can avoid the preparation of stannylated monomers, which themselves require caution in handling and have associated problems of instability. In fact, direct arylation polycondensation of bithiazole-based monomers provided a series of conjugated polymers with high molecular weight.[19–22] In some cases, only low-molecular-weight polymers were obtained due to the low solubility of the target polymers in the reaction solvent, N,N-dimethylacetamide (DMAc).[21,22] To overcome this issue, investigation of reaction conditions was the primary objective of this study. In addition, we evaluated the accuracy of repeating structures of the polymers synthesized under the established reaction conditions. Finally, the structure–property relations of the polymers were investigated in terms of absorption properties, energy levels, crystallinity, and semiconducting properties for providing basic insight into bithiazole-based polymers.

EXPERIMENTAL PROCEDURE

Materials

Pd(OAc)$_2$, chlorobenzene (CB) and 1,8-diiodooctane (DIO), and other chemicals were received from commercial suppliers and used without further purification. Pd(PCy$_3$)$_2$ was purchased from Aldrich and stored under N$_2$ atmosphere at 0 °C. Anhydrous DMAc was purchased from Kanto Chemical and used as a dry solvent. N,N-diethylpropanamide was dried over molecular sieves and degassed by freeze-pump-thaw cycles prior to use. 4,4′-Bis(2-octyldodecyl)-2,2′-bithiazole,[21]

5,5′-dibromo-2,2′-bithiazole,[23] 4,4′-dinonyl-2,2′-bithiazole,[24] and 2,6-dibromo-4,8-bis(2-octyldodecyloxy)benzo[1,2-b:4,5-b']dithiophene[25] were prepared according to the literature methods. A synthetic procedure of 2,6-dibromo-4,8-bis(2-octyldodecyl)benzo[1,2-b:4,5-b']dithiophene was described in supporting information. Poly(3,4-ethylenedioxythiophene)-poly(styrenesulfonate) (PEDOT:PSS, CLEVIOS P VP AI 4083) was purchased from Heraeus. PC$_{70}$BM (purity 99%) was purchased from Solenne.

General Measurements and Characterization

NMR spectra were recorded by AVANCE-400 and AVANCE-600 NMR spectrometer (Bruker). Gel permeation chromatography (GPC) measurements were carried out using a prominence GPC system (SHIMADZU) equipped with polystyrene gel columns, using CHCl$_3$ as the eluent after calibration with polystyrene standards (40 °C). High-temperature GPC measurements (140 °C) were carried out using a HLC-8321 GPC/HT (TOSOH) using o-dichlorobenzene (o-DCB) as the eluent after calibration with polystyrene standards. Matrix Assisted Laser Desorption/Ionization Mass (MALDI-TOF-MS) spectra were recorded on a MALDI TOF/TOF 5800 (AB SCIEX) in a linear mode using dithranol as matrix. Ultraviolet-visible (UV-vis) absorption spectra were recorded using a V-630 spectrometer (JASCO). X-ray diffraction (XRD) patterns were recorded at 298 K on a Rigaku model MultiFlex X-ray diffractometer with a Cu$K\alpha$ radiation source. The HOMO energy levels were estimated by photoelectron yield spectroscopy (PYS) using an AC-3 spectrometer (Riken Keiki). Atomic force microscopy (AFM) images were obtained using Nanocute (SII Nano Technology, Inc.). The thermal properties were measured on an EXSTAR TG/DTA6300 instrument. DFT calculations were performed at the B3LYP/6-31G(d) level with the Gaussian09 Rev. D.01 program. All the manipulations for the reactions were carried out under a nitrogen atmosphere using a glove box or standard Schlenk technique.

Synthesis of P1

A mixture of Pd(PCy$_3$)$_2$ (6.6 mg, 0.010 mmol), 1-adamantanecarboxylic acid (10.6 mg, 0.059 mmol), K$_2$CO$_3$ (67.2 mg, 0.49 mmol), 5,5′-dibromo-2,2′-bithiazole (63.9 mg, 0.20 mmol), 4,4′-di(2-octyldodecyl)-2,2′-bithiazole (143 mg, 0.20 mmol) was stirred in N,N-diethylpropanamide (2.0 mL) at 100 °C for 48 h under nitrogen atmosphere. After cooling to room temperature, the mixture was poured into aqueous solution of ethylenediaminetetraacetic acid disodium salt (pH = 8). The suspension was stirred for 1 h at room temperature. The precipitates were separated by filtration and washed with 10% HCl solution, distilled water, methanol, and hexane. The remaining solid was extracted with CHCl$_3$ by sonication and stirring at room temperature. The solution was filtered, concentrated and reprecipitated into methanol. The precipitates were collected by filtration and dried under reduced pressure. **P1** was isolated as dark red solid in 43% yield as a hexane-insoluble and

CHCl$_3$-soluble fraction. M_n = 35000, M_w/M_n = 3.21. ^{1}H NMR (600 MHz, C$_2$D$_2$Cl$_4$, 373 K): δ 7.94 (s, 2H), 2.89 (br, 4H), 2.05 (m, 2H), 1.43-1.18 (br, 64H), 0.85 (m, 12H). ^{13}C{^{1}H} NMR (150 MHz, C$_2$D$_2$Cl$_4$, 373 K): δ 161.36, 159.11, 156.92, 143.56, 131.03, 124.25, 38.35, 35.48, 34.31, 34.09, 32.06, 30.16, 29.79, 29.74, 29.43, 26.95, 22.76, 14.11 (8 signals of the alkyl group were overlapped). Anal. Calcd for C$_{52}$H$_{84}$N$_4$S$_4$: C, 69.90; H, 9.48; N, 6.27; S, 14.35; Br, 0.00. Found: C, 69.05; H, 9.86; N, 6.32; S, 14.42; Br, 0.14.

Synthesis of P2

A mixture of Pd(PCy$_3$)$_2$ (5.0 mg, 0.0075 mmol), 1-adamantanecarboxylic acid (8.1 mg, 0.045 mmol), K$_2$CO$_3$ (51.8 mg, 0.38 mmol), 2,6-dibromo-4,8-bis(2-octyldodecyloxy)benzo[1,2-*b*:4,5-*b'*] dithiophene (141.2 mg, 0.15 mmol), 4,4′-dinonyl-2,2′-bithiazole (63.1 mg, 0.15 mmol) in *N,N*-diethylpropanamide (1.5 mL) was stirred at 100 °C for 48 h under nitrogen atmosphere. Then, a solution of 4,4'-dinonyl-2,2'-bithiazole (31.5 mg, 0.075 mmol) in *N,N*-diethylpropanamide (1.5 mL) was added to the reaction mixture. After the reaction at 100 °C for 24 h, **P2** was isolated as a hexane-insoluble and CHCl$_3$-soluble fraction in 51% by the same purification procedure for **P1**. M_n = 47000, M_w/M_n = 3.61. ^{1}H NMR (600 MHz, C$_2$D$_2$Cl$_4$, 373 K): δ 7.58 (s, 2H), 4.26 (br, 4H), 3.07 (br, 4H), 1.97-1.82 (br, 4H), 1.65 (br, 2H), 1.57-1.17 (m, 88H) 0.86 (m, 18H). ^{13}C{^{1}H} NMR (150 MHz, C$_2$D$_2$Cl$_4$, 373 K): δ 159.01, 156.50, 144.59, 133.38, 132.30, 130.08, 128.14, 120.64, 77.17, 39.81, 32.05, 31.91, 30.89, 30.28, 29.84, 29.78, 29.71, 29.68, 29.56, 29.44, 27.35, 22.75, 14.09 (14 signals of the alkyl group were overlapped). Anal. Calcd for C$_{74}$H$_{122}$N$_2$O$_2$S$_4$: C, 74.07; H, 10.25; N, 2.33; S, 10.69; Br, 0.00. Found: C, 72.94; H, 10.43; N, 2.45; S, 10.56; Br, 0.11.

Synthesis of P3

P3 was synthesized by the same procedure for **P2** in a 0.18 mmol scale with 2,6-dibromo-4,8-bis(2-octyldodecyl)benzo[1,2-*b*:4,5-*b'*]dithiophene (163.9 mg, 0.18 mmol) instead of 2,7-dibrom-4,8-bis(2-octyldodecyloxy)benzo[1,2-*b*:4,5-*b'*]dithiophene. **P3** was isolated as a hexane-insoluble and CHCl$_3$-soluble fraction in 85% yield. M_n = 49000, M_w/M_n = 4.61. ^{1}H NMR (600 MHz, C$_2$D$_2$Cl$_4$, 373 K): δ 7.57 (s, 2H), 3.09 (br, 8H), 2.13 (br, 2H), 1.90 (br, 4H), 1.53-1.15 (m, 88H), 0.855 (m, 18H). ^{13}C{^{1}H} NMR (150 MHz, C$_2$D$_2$Cl$_4$, 373K): δ 158.83, 156.18, 139.11, 137.59, 133.22, 128.81, 128.65, 122.50, 39.22, 38.86, 34.77, 32.05, 30.99, 30.20, 29.78, 29.73, 29.69, 29.59, 29.43, 27.12, 22.75. 14.08 (15 signals of the alkyl group were overlapped). Anal. Calcd for C$_{74}$H$_{122}$N$_2$S$_4$: C, 76.09; H, 10.53; N, 2.40; S, 10.98; Br, 0.00. Found: C, 75.40; H, 10.88; N, 2.39; S, 11.33; Br, 0.00.

Fabrication and characterization of OPV cells

The OPV cells were fabricated in the following configuration: ITO/PEDOT:PSS/bulk heterojunction

(BHJ) layer/LiF/Al. The patterned ITO (conductivity: 10 Ω/square) glass was precleaned in an ultrasonic bath of acetone and ethanol, and then treated in an ultraviolet-ozone chamber. A thin layer (40 nm) of PEDOT:PSS was spin-coated onto the ITO at 3,000 rpm and air-dried at 110 °C for 10 min on a hot plate. The substrate was then transferred to a N_2-filled glove box where it was re-dried at 110 °C for 10 min on a hot plate. A CB solution (3% DIO) of the **P2** and $PC_{70}BM$ blended in 1:2 or 1:4 ratio was subsequently spin-coated onto the PEDOT:PSS surface to form the BHJ layer. The substrates with the BHJ layers were dried for 10 min at 110 °C for the film spin-casted from the CB solution. LiF (1 nm) and Al (80 nm) were then deposited onto the active layer by conventional thermal evaporation at a chamber pressure lower than 5×10^{-4} Pa, which provided the devices with an active area of 5×2 mm^2. The thicknesses of BHJ and PEDOT:PSS layers were measured using an automatic microfigure measuring instrument (SURFCORDER ET200, Kosaka Laboratory, Ltd.). The current density-voltage (*J-V*) curves were measured using an ADCMT 6244 DC voltage current source/monitor under AM 1.5 solar-simulated light irradiation of 100 mW cm^{-2} (OTENTO-SUN III, Bunkoh-Keiki Co.). The external quantum efficiency (EQE) and the internal quantum efficiency (IQE) were measured using an SM-250 system (Bunkoh-Keiki Co., Ltd.) with an integrating sphere to determine the reflectance (*R*) of the BHJ OPVs for estimating IQE=EQE/(1–*R*).

RESULTS AND DISCUSSION

Optimization of reaction conditions

With the aim of investigating synthetic conditions for a conjugated polymer with low solubility, direct arylation polycondensation of 4,4′-bis(2-octyldodecyl)-2,2′-bithiazole with 5,5′-dibromo-2,2′-bithiazole was selected as a target reaction. The corresponding polymer (**P1**) was supposed to have low solubility in polar solvents owing to its planar structure and the interchain interactions of the bithiazole units (Table 1).[26,27] Under the previously reported conditions using DMAc,[19–22] only oligomeric products were obtained as expected (Entry 1, Table 1). In Entry 2, a reaction at higher temperature (120 °C) was conducted to increase the reaction rate and the amount of dissolved polymer during the reaction. In this reaction, a Pd(0) precatalyst with phosphine ligands was used to stabilize a Pd catalyst at high temperature, instead of the reported phosphine-free catalyst.[13] The molecular weight of the obtained polymer somewhat increased to a value of 6000 (Entry 2), but the product was still soluble in hexane at room temperature. The addition of an aromatic solvent, *m*-xylene, did not improve molecular weight (Entry 3). Upon changing the solvent from DMAc to *N,N*-diethylpropanamide, the reaction afforded a hexane-insoluble product (60%), which is a relatively high-molecular-weight fraction (Entry 4). In terms of Pd(0) precatalyst, Pd(PCy$_3$)$_2$ was a suitable precursor for this reaction (Entry 4-6). In *N,N*-diethylpropanamide, a reaction at 100 °C provided a high-molecular-weight polymer with M_n = 35000 (Entry 7). A reaction temperature of 90 °C was insufficient for the formation of a high-molecular-weight polymer (Entry

8). Based on these results, the reaction conditions used for Entry 7 were determined to be the most suitable conditions for the synthesis of **P1** in polar solvent. PCy_3 has been reported to be an efficient supporting ligand for a Pd catalyst in direct arylation reactions.[28] The use of the Pd(0) precursor, $Pd(PCy_3)_2$, instead of a Pd(II) precursor, may lead to a high initiation efficiency of catalysis.[29] *N*,*N*-diethylpropanamide showed better solubilizing properties to **P1** than DMAc at 100 °C, presumably due to the additional methylene moieties in *N*,*N*-diethylpropanamide (Figure S1). The high solubilizing property of *N*,*N*-diethylpropanamide to **P1** results in the formation of high-molecular-weight polymer. Thompson *et al.* also reported that *N*,*N*-diethylpropanamide was available in synthesis of poly(3-hexylthiophene) using a direct arylation reaction.[30] Toluene was not appropriate solvent for this reaction system (Table S1) although toluene was utilized for direct arylation polycondensation of several electron deficient monomers.[31,32] A high-temperature GPC measurement (140 °C) for the sample from entry 7 revealed somewhat lower molecular weight (M_n = 22000) than the measurement at 40 °C (M_n = 35000). This observation indicates aggregation of **P1** at around room temperature. The aggregation behavior was evaluated by UV-vis absorption spectroscopy as described later.

Table 1 Results of polycondensation reactions [a]
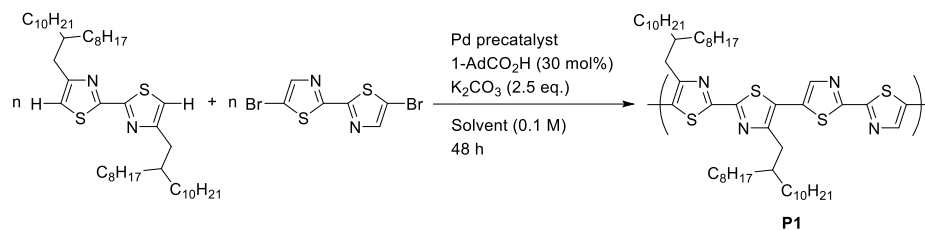
Entry	Catalyst	Temp. / °C	Solvent [g]	Hexane soluble part [b]		CHCl$_3$ soluble part [c]	
				Yield / %	M_n [d] (M_w/M_n)	Yield / %	M_n [d] (M_w/M_n)
1	Pd(OAc)$_2$ [e]	100	DMAc	79	2700 (1.19)		
2	Pd(PAr$_3$)$_3$ [f]	120	DMAc	86	6000 (1.88)		
3	Pd(PAr$_3$)$_3$ [f]	120	DMAc /m-xylene [h]	77	5300 (2.28)		
4	Pd(PAr$_3$)$_3$ [f]	120	DEPA	20	6000 (2.52)	62	17000 (2.86)
5	Pd(Pt-Bu$_3$)$_2$	120	DEPA	99	12000 (2.80)		
6	Pd(PCy$_3$)$_2$	120	DEPA	52	11000 (3.34)	44	26000 (3.01)
7	Pd(PCy$_3$)$_2$	100	DEPA	42	18000 (2.85)	43	35000 (3.21)
8	Pd(PCy$_3$)$_2$	90	DEPA	57	19000 (1.40)		

[a] Reactions were carried out using a Pd precatalyst (5 mol%), 1-AdCOOH (30 mol%), and K$_2$CO$_3$ (2.5 equiv), [b] Methanol-insoluble and hexane-soluble fraction, [c] Hexane-insoluble and CHCl$_3$-soluble fraction, [d] Estimated by GPC calibrated on polystyrene standards using CHCl$_3$ as an eluent at 40 °C, [e] 2 mol% of Pd precatalyst, [f] PAr$_3$ = tris[3,5-bis(trifluoromethyl)phenyl]phosphine, [g] DMAc = N,N-dimethylacetamide, DEPA = N,N-diethylpropanamide, [h] 1:1 mixture of DMAc and m-xylene.

Characterization of polymer structure

The structure of **P1** was evaluated by ^{1}H NMR and MALDI-TOF-MS. Figure 1 shows the ^{1}H NMR spectrum of **P1** obtained from Entry 7 in Table 1. In addition to the signals corresponding to the repeating unit (7.94, 2.89, and 2.05 ppm), signals of the terminal 4,4′-bis(2-octyldodecyl)bithiazole unit were observed at 6.94, 2.75 and 1.84 ppm. The small signal at 8.01 ppm could be assigned to a linkage of the non-substituted bithiazole unit, which was estimated from the chemical shift of 5,5′-bithiazole.[33] The non-alternating structure was caused by a homo-coupling reaction of the C-Br moieties of 5,5′-dibromo-2,2′-bithiazole, which is known to be a common side reaction in direct arylation polycondensation.[34–36] The signal intensity corresponding to the homo-coupling defect

depends on the reaction conditions (Figure S2). The polymer from Entry 7 shows a relatively small amount of defects compared with those from Entry 4 and 6 (Table 1). These results indicate that the use of PCy$_3$ and a low reaction temperature suppress the side reaction. In direct arylation, the homo-coupling reaction of arylbromide is considered to occur via the transmetalation of aryl-Pd intermediates after oxidative addition of the arylbromide.[29,37] PCy$_3$ may suppress the undesired transmetalation of the intermediates due to its bulkiness and strong coordination ability. In evaluating the side reaction, MALDI-TOF-MS shows similar trends to the results of ^{1}H NMR; the mass spectrum of the polymer from Entry 7 shows relatively low intensity peaks corresponding to the defect structure (Figure S3). The structure from C-H/C-H homo-coupling was also detected in the mass spectrum, although the ^{1}H NMR spectrum did not show the presence of the structure, presumably due to overlapping signals with those of the terminal structures.
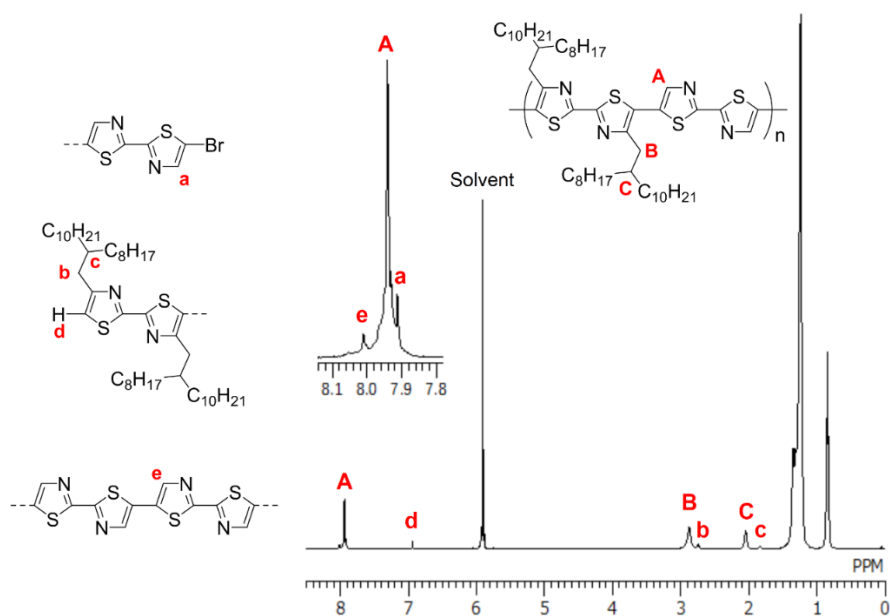

Figure 1. ^{1}H NMR spectrum of **P1** (Entry 7 in Table 1) (600 MHz, C$_2$D$_2$Cl$_4$, 373 K).

8

Synthesis of donor-acceptor polymers

On the basis of the established reaction conditions, bithiazole-based donor-acceptor (D-A) polymers were synthesized via direct arylation of 4,4′-dinonyl-2,2′-bithiazole with dibromobenzodithiophene derivatives to confirm the application range of the reaction conditions (Table 2). Dibromoaromatic monomers, 2-octyldodecyloxy- and 2-octyldodecyl-substituted dibromobenzodithiophenes were selected for preparation of D-A polymers with different electronic properties. Both of the reactions with 2-octyldodecyloxy- and 2-octyldodecyl-substituted dibromobenzodithiophenes afforded high-molecular-weight polymers (**P2** and **P3**) and in reasonable yields. In the case of the 2-octyldodecyloxy-substituted dibromobenzodithiophene, a small amount of CHCl$_3$-insoluble products were obtained, presumably due to low solubility caused by stronger interchain D-A interactions. Previous reports have shown that a polycondensation reaction using Stille cross-coupling can afford an analogous polymer to **P2** with a molecular weight of 7000.[7] The higher molecular weight of **P2** proves that the established reaction conditions are useful for the synthesis of D-A polymers. Recently, Wakioka and Ozawa *et al.* reported direct arylation polycondensation of a bithiazole monomer in THF using their original catalytic system.[38] Since this reaction also afforded a high-molecular-weight polymer, THF is the other option for the synthesis of bithiazole-based polymers.

Table 2 Synthesis of **P2** and **P3**
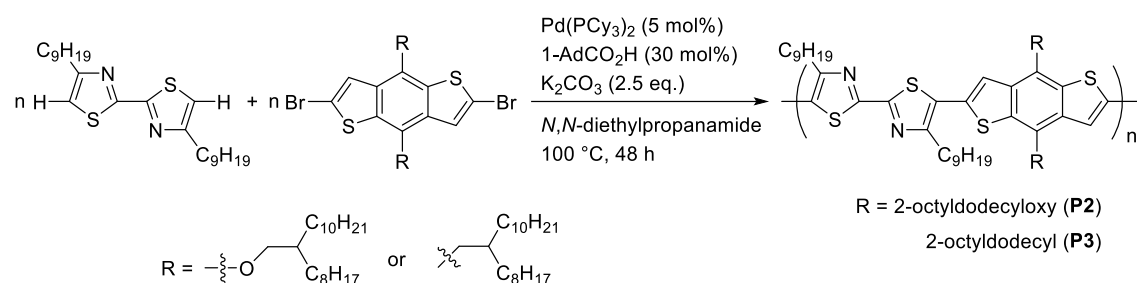
Polymer	R	Hexane soluble part [a]		CHCl$_3$ soluble part [b]		
		Yield / %	M_n [c] (M_w/M_n)	Yield / %	M_n [c] (M_w/M_n)	M_n [d] (M_w/M_n)
P2	2-Octyldodecyloxy	24	22000 (2.11)	51 [e]	47000 (3.61)	28000 (2.49)
P3	2-Octyldodecyl	10	15000 (1.30)	85	49000 (4.61)	28000 (2.49)

[a] Methanol-insoluble and hexane-soluble fraction. [b] Hexane-insoluble and CHCl$_3$-soluble fraction. [c] Estimated by GPC calibrated on polystyrene standards using CHCl$_3$ as an eluent at 40 °C. [d] Estimated by GPC calibrated on polystyrene standards using *o*-DCB as an eluent at 140 °C. [e] Insoluble products in CHCl$_3$ were also obtained.

9

The ^{1}H NMR spectrum of **P2** shows relatively small signals of the terminal bithiazole structure in comparison with **P1**, owing to high molecular weight of **P2** (Figure 2). Three signals of the debrominated benzodithiophene terminal were observed at 7.67, 7.46, and 7.36 ppm, with a reasonable coupling pattern. The homo-coupling structure of the benzodithiophene unit was also detected at 7.54 ppm, with low intensity.[39] In **P3**, similar signal patterns were observed in the ^{1}H NMR spectrum (Figure S4). MALDI-TOF-MS spectra showed that the alternative structures were dominant in both **P2** and **P3** (Figures S5 and S6).
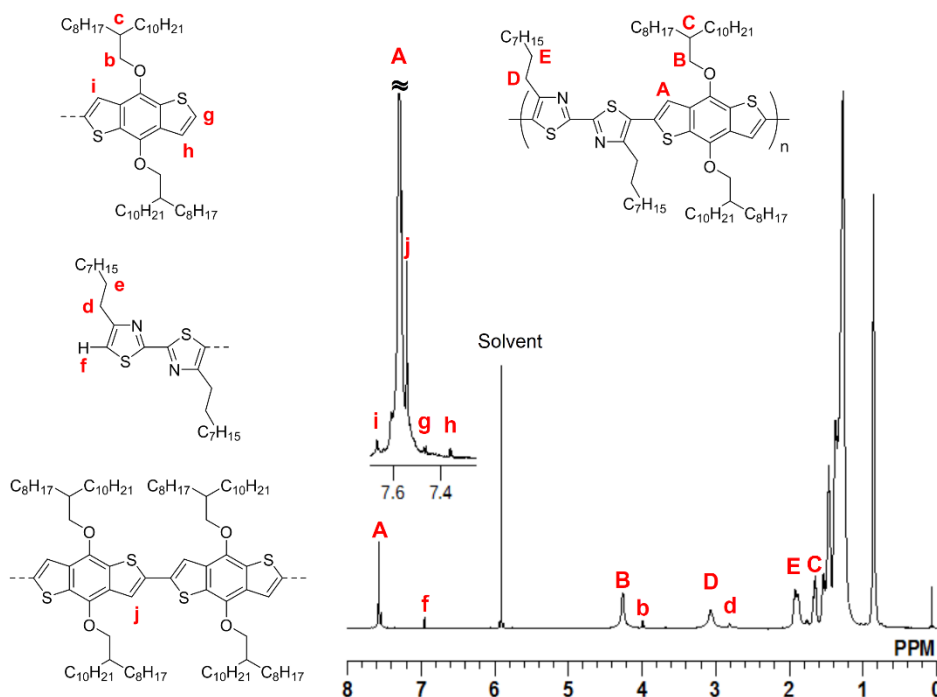

Figure 2. ^{1}H NMR spectrum of **P2** (600 MHz, $C_2D_2Cl_4$, 373 K).

Absorption properties

Absorption maxima of **P1** – **P3** appear at around 500 nm in the solution state (Figures 3a-c and Table 3). These absorption bands are associated with shoulders in a longer wavelength region. The shoulders are likely to be a result of aggregation of the polymer in solution, because TD-DFT calculations for model compounds of **P1** – **P3** showed no transition in the long wavelength region (Figure 4). The hypothesis of aggregation is also supported by the enhancement of the shoulder bands in the film state. To investigate the aggregation behavior, variable temperature absorption spectra were measured from 30 °C to 80 °C (Figures 3d-f). These spectra clearly showed blue shifts of absorption at high temperature, proving dissociation of aggregates.[40] The shapes of the absorption spectra at 80 °C are in good agreement with those of the estimated absorption spectra by the TD-DFT calculations (Figure 4). At 80 °C, **P1** – **P3** all possess a similar wavelength of absorption

maxima, although **P2** and **P3** are expected to show long-wavelength absorption compared with **P1** owing to the D-A structures of **P2** and **P3**. A weak acceptor property of the bithiazole unit might result in a small contribution of charge transfer absorption.[21] Indeed, the TD-DFT calculations showed a large contribution from a π-π* transition from HOMO to LUMO in each polymer rather than a charge transfer transition (Figure 4).
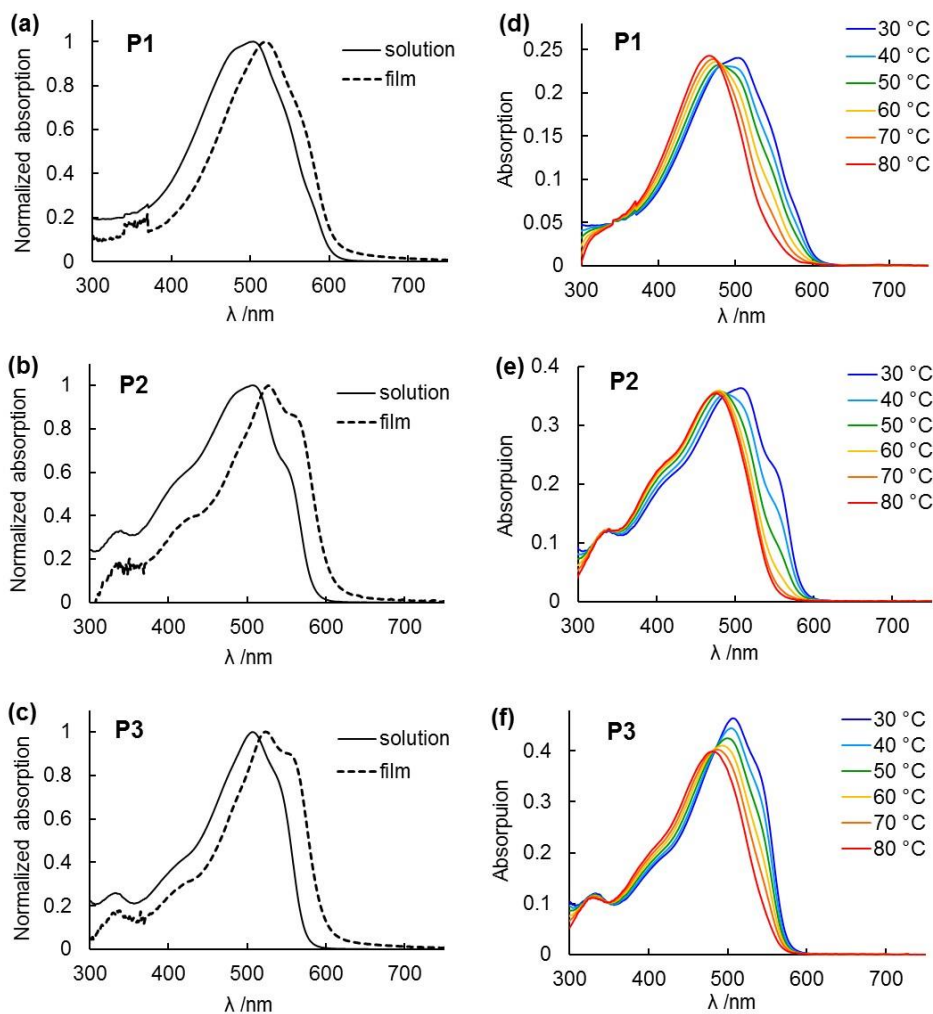

Figure 3. (a)-(c) UV-vis absorption spectra of **P1** – **P3** in the solution state (toluene, 30 °C, 1.0×10⁻⁵ M) and the film state. (d)-(f) Variable temperature absorption spectra of **P1** – **P3** in toluene (30 – 80 °C, 1.0×10⁻⁵ M).

Table 3 Absorption properties

Polymer	Solution [a]		Calculation [b]	Film	
	λ_{max} / nm at 30 °C	λ_{max} / nm at 80 °C	λ_{max} / nm	λ_{max} / nm	λ_{onset} [c] / nm
P1	504	466	517	520	602
P2	507	476	498	527	603
P3	507	480	505	523	600

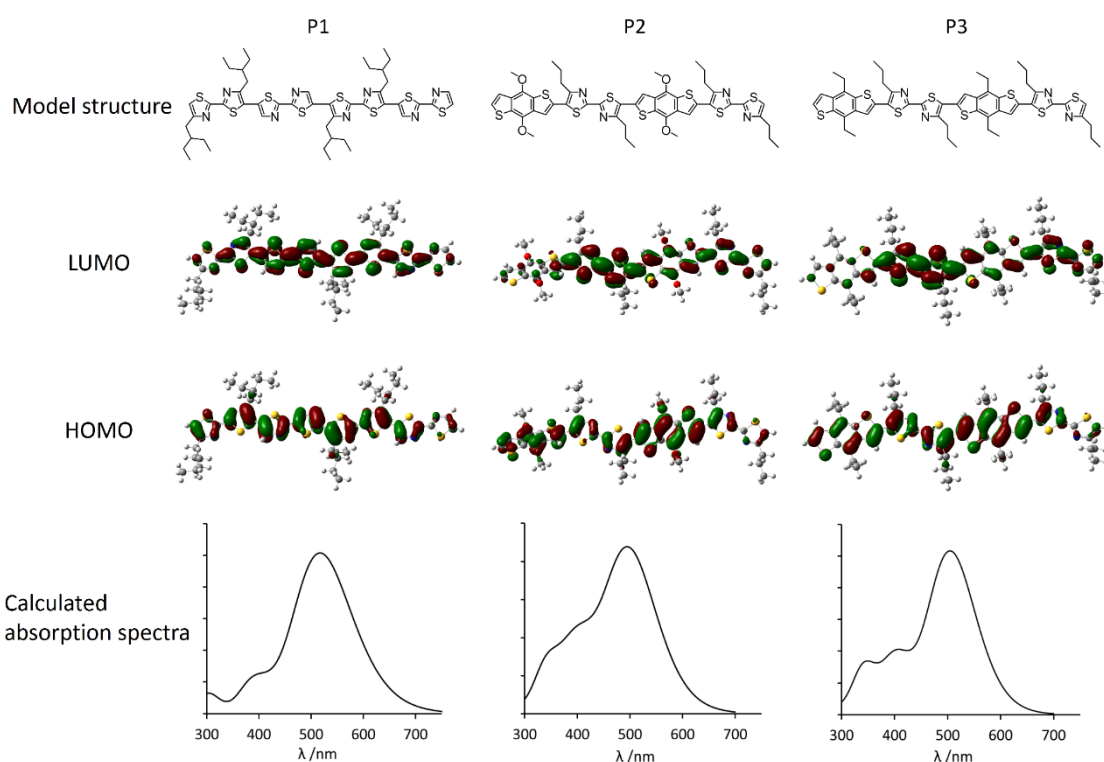[a] In toluene (1.0×10⁻⁵ M), [b] Calculated by TD-DFT, [c] Absorption onset.

Figure 4. HOMO and LUMO distribution of model compounds for **P1** – **P3**, and calculated absorption spectra obtained by TD-DFT calculation.

Physical properties

The physical properties of **P1**–**P3** are summarized in Table 4. In contrast to similar absorption properties and band gaps in **P1**–**P3**, the energy levels reasonably reflect their chemical structures (Figure S17).[21,41] Photoelectron yield spectroscopy showed a lower HOMO level of **P1** than those of **P2** and **P3**, due to the acceptor–acceptor structure of **P1**. The presence of an electron-donating oxygen atom in the side chain of **P2** contributes the slightly higher HOMO level when compared with **P3**. To evaluate crystallinity in the film state, XRD analysis was conducted on **P1** – **P3** before

12

and after annealing at 200 °C (Figure 5, Table 4). In all polymers, the annealing treatments sharpened the diffraction peaks. After annealing, **P1** showed diffraction peaks corresponding to a lamellar structure up to the fourth order. A diffraction peak of a π-π stacking structure was not detected. Similar diffraction patterns were reported in bithiazole-rich conjugated polymers.[4,5,27] In contrast, **P2** shows a strong diffraction peak in a high-angle region ($2\theta = 23.20°$) corresponding to a π-π stacking structure. The lamellar diffraction peak was relatively small (3.67°). In addition, a diffraction peak at 5.69° ($d = 15.51$ Å) was detected with a second-order diffraction at 11.17°. Because the distance of the repeating unit of **P2** was estimated as 15.9 Å by the DFT calculation, it was proposed that these diffractions may be the result of a periodic structure in a main chain direction. Similar observations have been reported in literature.[42,43] **P3** shows diffractions from both lamellar and stacking structures.

Table 4 Physical properties

Polymer	E_g^{opt} [a] / eV	HOMO [b] / eV	LUMO [c] / eV	T_{d5} [d] / °C	Diffraction peak (2θ) [e]
P1	2.06	-5.99	-3.93	405	4.17, 8.34, 12.52, 16.87
P2	2.06	-5.40	-3.34	312	3.67, 5.69, 11.17, 23.20
P3	2.07	-5.49	-3.42	410	3.61, 5.60, 7.15, 22.33

[a] Optical bandgap from the absorption onset in the film state, [b] HOMO from photoelectron yield spectroscopy, [c] LUMO = HOMO- E_g^{opt}, [d] The 5% weight-loss temperatures under inert atmosphere, [e] Diffraction peaks from XRD after annealing at 200 °C.
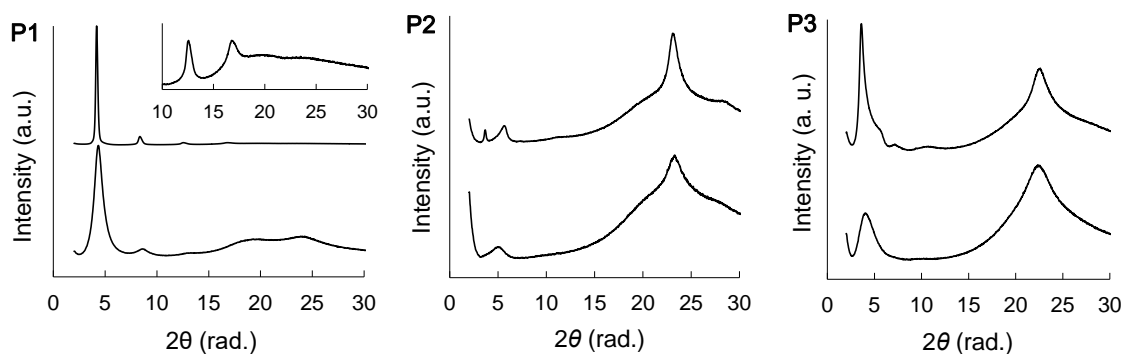

Figure 5. X-ray diffraction patterns of **P1**–**P3** before (bottom) and after annealing (top).

OPV characteristics

As the energy levels of **P2** and **P3** looked promising, these polymers were evaluated as BHJ OPV materials. BHJ OPVs were fabricated with $PC_{70}BM$ as the acceptor material and blend ratios of 1:2 or 1:4, using various solvents (Tables 5 and S2). The OPV with **P2**:$PC_{70}BM$ at a 1:4 mixing ratio

using CB as solvent yielded a PCE of 0.51% (Entry 1, Table 5). This PCE increased to 1.03% upon addition of 3% DIO in CB (Entry 2). The surface morphology of the active layers was evaluated using AFM (Figure 6). In contrast to a smooth surface of **P2** (Figure 6a), a rough surface of the BHJ film with **P2** and $PC_{70}BM$ was observed, indicating substantial phase separation (Figure 6b). The pronounced phase separation certainly reduced the heterojunction interface area for exciton dissociation and consequently led to the low J_{sc} of BHJ OPVs. Since the addition of 3% DIO in CB decreased the domain size (Figure 6c), the increase in PCE was likely to be the result of an improvement in phase separation. **P3** showed a similar trend to **P2**. Because of strong intermolecular interaction of the bithiazole units, the control of aggregation behavior is crucial for the improvement of PCE in bithiazole-based polymer materials.

Table 5 OPV characteristics [a]

Entry	Polymer	Solvent [b]	Thickness / nm	J_{sc} / mAcm^{-2}	V_{oc} / V	FF	PCE /%
1	**P2**	CB	88	1.55 ± 0.04	0.78 ± 0.03	0.425 ± 0.006	0.51 ± 0.04
2	**P2**	CB + DIO 3%	87	2.99 ± 0.12	0.75 ± 0.03	0.46 ± 0.01	1.03 ± 0.05
3	**P3**	CB	78	0.98 ± 0.09	0.70 ± 0.04	0.39 ± 0.08	0.28 ± 0.09
4	**P3**	CB + DIO 3%	80	2.40 ± 0.09	0.67 ± 0.03	0.45 ± 0.02	0.74 ± 0.07

[a] The average values with standard deviations were calculated from the results of three or more OPV samples. OPV configuration: ITO/PEDOT:PSS (40 nm)/**P2**–**P3**:$PC_{70}BM$ (1:4)/LiF (1 nm)/Al (80 nm). [b] Chlorobenzene (CB), 1,8-diiodooctane (DIO).
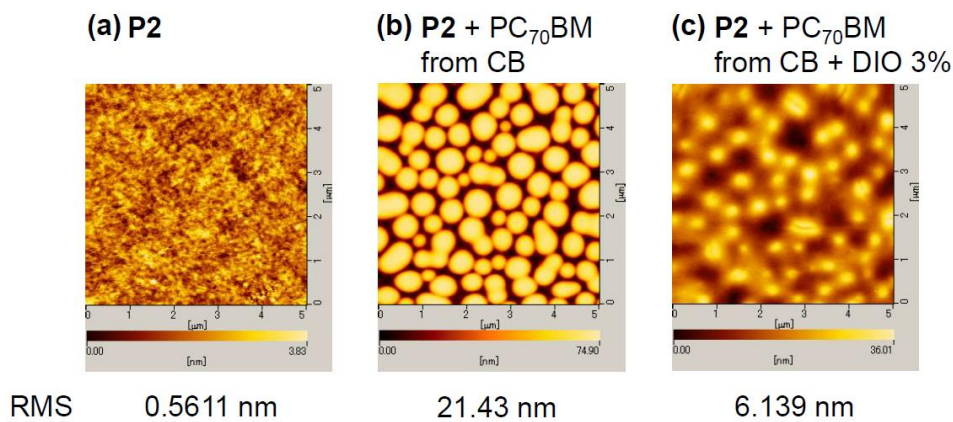

(a) P2   **(b) P2** + $PC_{70}BM$ from CB   **(c) P2** + $PC_{70}BM$ from CB + DIO 3%

RMS   0.5611 nm   21.43 nm   6.139 nm

Figure 6. AFM images (5 × 5 μm^2) of **P2** and **P2**:$PC_{70}BM$ (1:4) with values of the root mean square (RMS) roughness.

CONCLUSION

The investigation of the reaction conditions of direct arylation polycondensation lead to the successful synthesis of bithiazole-based crystalline polymers having low solubility. The choice of a suitable solvent, *N*,*N*-diethylpropanamide, facilitated smooth coupling reactions along with the prevention of precipitation of growing polymers as the reaction progressed. The bithiazole-based polymer shows aggregation behavior even in the dilute solution state (1×10^{-5} M). This aggregation behavior produced high crystallinity, evidenced by XRD analysis. The control of aggregation was a key factor for increasing the PCE of the BHJ OPVs with the bithiazole-based conjugated polymers. This study expanded the application range of direct arylation polycondensation for the preparation of various crystalline polymers having low solubility. In addition, the detailed investigation of the structure–property relationships provides basic insights into the molecular design of conjugated polymer materials.

CONFLICT OF INTEREST

The authors declare no conflict of interest.

References

1. Lin, Y., Fan, H., Li, Y. & Zhan, X. Thiazole-based organic semiconductors for organic electronics. *Adv. Mater.* **24,** 3087–3106 (2012).

2. Ando, S., Murakami, R., Nishida, J. I., Tada, H., Inoue, Y., Tokito, S. & Yamashita, Y. n-Type organic field-effect transistors with very high electron mobility based on thiazole oligomers with trifluoromethylphenyl groups. *J. Am. Chem. Soc.* **127,** 14996–14997 (2005).

3. Balan, B., Vijayakumar, C., Saeki, A., Koizumi, Y. & Seki, S. p/n Switching of ambipolar bithiazole-benzothiadiazole-based polymers in photovoltaic cells. *Macromolecules* **45,** 2709–2719 (2012).

4. Liu, J., Zhang, R., Osaka, I., Mishra, S., Javier, A. E., Smilgies, D. M., Kowalewski, T. & McCullough, R. D. Transistor paint: Environmentally stable *N*-alkyldithienopyrrole and bithiazole-based copolymer thin-film transistors show reproducible high mobilities without

annealing. *Adv. Funct. Mater.* **19,** 3427–3434 (2009).

5. Kim, D. H., Lee, B. L., Moon, H., Kang, H. M., Jeong, E. J., Park, J. Il, Han, K. M., Lee, S., Yoo, B. W., Koo, B. W., Kim, J. Y., Lee, W. H., Cho, K., Becerril, H. A. & Bao, Z. Liquid-crystalline semiconducting copolymers with intramolecular donor-acceptor building blocks for high-stability polymer transistors. *J. Am. Chem. Soc.* **131,** 6124–6132 (2009).

6. Li, K., Huang, J., Hsu, Y., Huang, P., Lin, J., Ho, K., Wei, K., Lin, H. & Chu, C. Tunable novel cyclopentadithiophene-based copolymers containing various numbers of bithiazole and thienyl units for organic photovoltaic cell applications. *Macromolecules* **42,** 3681–3693 (2009).

7. Yang, M., Peng, B., Liu, B., Zou, Y., Zhou, K., He, Y., Pan, C. & Li, Y. Synthesis and photovoltaic properties of copolymers from benzodithiophene and thiazole. *J. Phys. Chem. C* **114,** 17989–17994 (2010).

8. Guo, X., Zhang, M., Huo, L., Cui, C., Wu, Y., Hou, J. & Li, Y. Poly(thieno[3,2-b]thiophene-alt-bithiazole): A D-A copolymer donor showing improved photovoltaic performance with indene-C_{60} bisadduct acceptor. *Macromolecules* **45,** 6930–6937 (2012).

9. Carsten, B., He, F., Son, H. J., Xu, T. & Yu, L. Stille polycondensation for synthesis of functional materials. *Chem. Rev.* **111,** 1493–1528 (2011).

10. Sakamoto, J., Rehahn, M., Wegner, G. & Schlüter, A. D. Suzuki polycondensation: Polyarylenes à la carte. *Macromol. Rapid Commun.* **30,** 653–687 (2009).

11. Huang, J. H., Li, K. C., Chien, F. C., Hsiao, Y. S., Kekuda, D., Chen, P., Lin, H. C., Ho, K. C. & Chu, C. W. Correlation between exciton lifetime distribution and morphology of bulk heterojunction films after solvent annealing. *J. Phys. Chem. C* **114,** 9062–9069 (2010).

12. Okamoto, K., Zhang, J., Housekeeper, J. B., Marder, S. R. & Luscombe, C. K. C-H arylation reaction: Atom efficient and greener syntheses of π-conjugated small molecules and macromolecules for organic electronic materials. *Macromolecules* **46,** 8059–8078 (2013).

13. Kuwabara, J. & Kanbara, T. Development of synthetic method for π conjugated polymers via direct arylation polycondensation. *J. Synth. Org. Chem., Jpn.* **72,** 1271–1278 (2014).

14. Segawa, Y., Maekawa, T. & Itami, K. Synthesis of extended π-systems through C-H activation. *Angew. Chem. Int. Ed.* **54,** 66–81 (2015).

15. Wang, Q., Takita, R., Kikuzaki, Y. & Ozawa, F. Palladium-catalyzed dehydrohalogenative polycondensation of 2-bromo-3-hexylthiophene: An efficient approach to head-to-tail poly(3-hexylthiophene). *J. Am. Chem. Soc.* **132,** 11420–11421 (2010).

16. Berrouard, P., Najari, A., Pron, A., Gendron, D., Morin, P. O., Pouliot, J. R., Veilleux, J. & Leclerc, M. Synthesis of 5-alkyl[3,4-c]thienopyrrole-4,6-dione-based polymers by direct heteroarylation. *Angew. Chem. Int. Ed.* **51,** 2068–2071 (2012).

17. Kuwabara, J., Yasuda, T., Choi, S. J., Lu, W., Yamazaki, K., Kagaya, S., Han, L. & Kanbara, T.

Direct arylation polycondensation: A promising method for the synthesis of highly pure, high-molecular-weight conjugated polymers needed for improving the performance of organic photovoltaics. *Adv. Funct. Mater.* **24,** 3226–3233 (2014).

18. Matsidik, R., Komber, H., Luzio, A., Caironi, M. & Sommer, M. Defect-free naphthalene diimide bithiophene copolymers with controlled molar mass and high performance via direct arylation polycondensation. *J. Am. Chem. Soc.* **137,** 6705 (2015).

19. Lu, W., Kuwabara, J. & Kanbara, T. Synthesis of 4,4′-dinonyl-2,2′-bithiazole-based copolymers via Pd-catalyzed direct C-H arylation. *Polym. Chem.* **3,** 3217–3219 (2012).

20. Choi, S. J., Kuwabara, J. & Kanbara, T. Microwave-assisted polycondensation via direct arylation of 3,4-ethylenedioxythiophene with 9,9-dioctyl-2,7-dibromofluorene. *ACS Sustain. Chem. Eng.* **1,** 878–882 (2013).

21. Kuramochi, M., Kuwabara, J., Lu, W. & Kanbara, T. Direct arylation polycondensation of bithiazole derivatives with various acceptors. *Macromolecules* **47,** 7378–7385 (2014).

22. Lu, W., Kuwabara, J., Kuramochi, M. & Kanbara, T. Synthesis of bithiazole-based crystalline polymers via palladium-catalyzed direct C-H arylation. *J. Polym. Sci. Part A Polym. Chem.* **53,** 1396–1402 (2015).

23. Jung, H., Yu, J., Jeong, E., Kim, J., Kwon, S., Kong, H., Lee, K., Woo, H. Y. & Shim, H. K. Synthesis and photovoltaic properties of cyclopentadithiophene-based low-bandgap copolymers that contain electron-withdrawing thiazole derivatives. *Chem. Eur. J.* **16,** 3743–3752 (2010).

24. Wong, W. Y., Wang, X. Z., He, Z., Chan, K. K., Djurišić, A. B., Cheung, K. Y., Yip, C. T., Ng, A. M. C., Yan, Y. X., Mak, C. S. K. & Chan, W. K. Tuning the absorption, charge transport properties, and solar cell efficiency with the number of thienyl rings in platinum-containing poly(aryleneethynylene)s. *J. Am. Chem. Soc.* **129,** 14372–14380 (2007).

25. Wang, H., Ding, Y., Lai, Y., Sun, Z., Liu, Y., Jiang, B., Chen, M., Yao, J., Liu, F. & Russell, T. P. Ethynylene-linked benzo[1,2-b:4,5-b′]dithiophene-alt-diketopyrrolopyrrole alternating copolymer: optoelectronic properties, film morphology and photovoltaic applications. *J. Mater. Chem. A* **3,** 12972–12981 (2015).

26. Nanos, J. I., Kampf, J. W. & Curtis, M. D. Poly(alkylbithiazoles): a new class of variable-bandgap, conjugated polymer. *Chem. Mater.* **7,** 2232–2234 (1995).

27. Yamamoto, T., Komarudin, D., Arai, M., Lee, B. L., Suganuma, H., Asakawa, N., Inoue, Y., Kubota, K., Sasaki, S., Fukuda, T. & Matsuda, H. Extensive studies on π-stacking of poly(3-alkylthiophene-2,5-diyl)s and poly(4-alkylthiazole-2,5-diyl)s by optical spectroscopy, NMR analysis, light scattering analysis, and X-ray crystallography. *J. Am. Chem. Soc.* **120,** 2047–2058 (1998).

28. Liégault, B., Lapointe, D., Caron, L., Vlassova, A. & Fagnou, K. Establishment of broadly applicable reaction conditions for the palladium-catalyzed direct arylation of

heteroatom-containing aromatic compounds. *J. Org. Chem.* **74,** 1826–1834 (2009).

29. Kuwabara, J., Sakai, M., Zhang, Q. & Kanbara, T. Mechanistic studies and optimisation of a Pd-catalysed direct arylation reaction using phosphine-free systems. *Org. Chem. Front.* **2,** 520–525 (2015).

30. Rudenko, A. E. & Thompson, B. C. The effect of amide solvent structure on the direct arylation polymerization (DArP) of 2-Bromo-3-hexylthiophene. *J. Polym. Sci. Part A Polym. Chem.* **53,** 2494–2500 (2015).

31. Wakioka, M., Nakamura, Y., Hihara, Y., Ozawa, F. & Sakaki, S. A highly efficient catalyst for the synthesis of alternating copolymers with thieno[3,4‑c]pyrrole-4,6-dione units via direct arylation polymerization. *Macromolecules* **47,** 626−631 (2014).

32. Kuwabara, J., Yamazaki, K., Yamagata, T., Tsuchida, W. & Kanbara, T. The effect of a solvent on direct arylation polycondensation of substituted thiophenes. *Polym. Chem.* **6,** 891–895 (2015).

33. Liu, Y., Shi, Q., Ma, L., Dong, H., Tan, J., Hu, W. & Zhan, X. Copolymers of benzo[1,2-b:4,5-b′]dithiophene and bithiazole for high-performance thin film phototransistors. *J. Mater. Chem. C* **2,** 9505–9511 (2014).

34. Kowalski, S., Allard, S. & Scherf, U. Scope and limitations of a direct arylation polycondensation scheme in the synthesis of PCPDTBT-type copolymers. *Macromol. Rapid Commun.* **36,** 1061–1068 (2015).

35. Lombeck, F., Matsidik, R., Komber, H. & Sommer, M. Simple synthesis of P(Cbz-alt-TBT) and PCDTBT by combining direct arylation with Suzuki polycondensation of heteroaryl chlorides. *Macromol. Rapid Commun.* **36,** 231–237 (2015).

36. Iizuka, E., Wakioka, M. & Ozawa, F. Mixed-Ligand Approach to Palladium-Catalyzed Direct Arylation Polymerization: Effective Prevention of Structural Defects Using Diamines. *Macromolecules* **49,** 3310−3317 (2016).

37. Wakioka, M., Nakamura, Y., Montgomery, M. & Ozawa, F. Remarkable ligand effect of P(2-MeOC$_6$H$_4$)$_3$ on palladium-catalyzed direct arylation. *Organometallics* **34,** 198–205 (2015).

38. Wakioka, M., Ishiki, S. & Ozawa, F. Synthesis of donor-acceptor polymers containing thiazolo[5,4-d]thiazole units via palladium-catalyzed direct arylation polymerization. *Macromolecules* **48,** 8382–8388 (2015).

39. Braunecker, W. A., Oosterhout, S. D., Owczarczyk, Z. R., Kopidakis, N., Ratcliff, E. L., Ginley, D. S. & Olson, D. C. Semi-random vs well-defined alternating donor-acceptor copolymers. *ACS Macro Lett.* **3,** 622–627 (2014).

40. Kong, H., Cho, S., Lee, D. H., Cho, N. S., Park, M. J., Jung, I. H., Park, J. H., Park, C. E. & Shim, H. K. The influence of electron deficient unit and interdigitated packing shape of new polythiophene derivatives on organic thin-film transistors and photovoltaic cells. *J. Polym. Sci. Part A Polym. Chem.* **49,** 2886–2898 (2011).

41.   Yasuda, T., Kuwabara, J., Han, L. & Kanbara, T. Photovoltaic properties of bithiazole-based polymers synthesized by direct C-H arylation. *J. Photopolym. Sci. Technol.* **29,** 347–352 (2016).

42.   Rivnay, J., Toney, M. F., Zheng, Y., Kauvar, I. V., Chen, Z., Wagner, V., Facchetti, A. & Salleo, A. Unconventional face-on texture and exceptional in-plane order of a high mobility n-type polymer. *Adv. Mater.* **22,** 4359–4363 (2010).

43.   Zhang, X., Bronstein, H., Kronemeijer, A. J., Smith, J., Kim, Y., Kline, R. J., Richter, L. J., Anthopoulos, T. D., Sirringhaus, H., Song, K., Heeney, M., Zhang, W., McCulloch, I. & DeLongchamp, D. M. Molecular origin of high field-effect mobility in an indacenodithiophene-benzothiadiazole copolymer. *Nat. Commun.* **4,** 2238/1–9 (2013).

Graphical Abstract
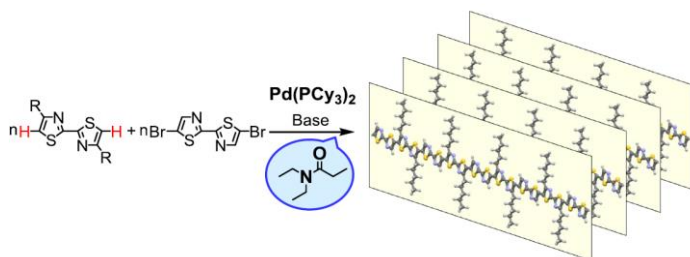
Direct arylation polycondensation using Pd(PCy$_3$)$_2$ as a precatalyst in *N,N*-diethylpropanamide as a reaction solvent afforded three kinds of the bithiazole-based conjugated polymers that were difficult to synthesize under previously reported conditions using *N,N*-dimethylacetamide. The obtained polymers showed aggregation properties and high crystallinity. The control of aggregation characteristics was a key factor for increasing the power conversion efficiency of organic photovoltaic devices fabricated from these polymers.